Parametric study for reducing emission characteristics using different computational schemes

IOP Conf. Series: Materials Science and Engineering **610** (2019) 012041 doi:10.1088/1757-899X/610/1/012041

Parametric study for reducing emission characteristics using different computational schemes

Hatem Kayed

Department of Mechanical Power Engineering, Cairo University, Egypt

E-mail. hatem_kayed@yahoo.com

Abstract: The present study numerically predicts emissions (NO_x & CO) characteristics issued from swirl burner using different computational schemes adopted in ANSYS 17.2. Various turbulence models were tested and compared in a structured grid having an average skewness of 0.04. RSM model shows the best results in predicting the central toroidal recirculation zone for such severe swirling flow (S>0.6). Three different schemes of combustion modeling were also tested and compared. Flamelet PDF model was preferred among other combustion models for its potential to consider non-equilibrium chemistry, where its choice was recommended form many studies in the literature. A radiation heat transfer analysis was carried out using P1 radiation model to account radiation effects in estimating NOx and CO concentrations. The effect of varying swirl ratio, excess air, diluting fuel with N_2 and CO_2, oxidizer preheating, and oxidizer composition on emissions (NO_x and CO) reduction strategy concluded that increasing the swirl number, excess air factor, and (N_2 and CO_2) mixing ratios have a considerable influence on NOx and CO emissions reduction. While increasing the preheating temperature, and the oxidizer Oxygen concentration leads to an increase the NOx and CO emissions. Hence, a considerable reduction in NO_x and CO formation was apparently observed by lowering the peak flame temperature less than 1800 K. These predicted outcomes are in agreement with measurements data published in the literature.

Keywords: NOx Emission, Turbulent Combustion, Modelling

1. Introduction

NO_X and CO emissions with considerable concentrations have severe impacts on human and the environment. Though, Temperature is the chief contributor for highly growing NOx emissions. 'Thermal NO_x' strongly depends on temperature since the 'NAN' bond in the molecular structure of Nitrogen is robust. NOx is considered the main source of photochemical smog that brings irritation of eyes, breathing difficulties and headaches, and also harms crops. The successive greenhouse warming leads to rising sea level and flooding as a result of backing up of rivers.

It is anticipated that emission regulations will be more restricted in the upcoming period, with roughly 80% drop from present levels in the next years [1]. Consequently, it is tremendously essential to find out and advance updated combustion methods. Understanding the turbulence-chemistry of combustion modeling assists in the enhancement of the processes which leads to lowest pollutants emitted. CFD) simulation of turbulent combustion is a crucial tool in design enhancement of burners and combustor performance.

Many combustion models and computational tools have been developed to predict emissions and combustion structure, one of which is flamelet that can have a great computational potential to efficiently predict turbulent combustion and emission characteristics [2,3]. Steady flamelet approach can be able to model local chemical nonequilibrium as a result of aerodynamic straining caused by turbulence field however, idle kinetic species, NOx, which doesn't interact rapidly as a result of turbulent straining should be simulated by unsteady flamelet approach, as their evolution relies on the development of molecular mixing and reactions [4]. Sanders et al. [5] carried out a laminar flamelet approach for turbulent flame and evaluated NO_x by calculating mass fraction transport-equation for NO. In this technique, chemical scales were decoupled, while solving the transport equation for NO was basically performed with frozen chemistry. Kim et al. [6] adopted unsteady flamelet and Conditional Moment Closure (CMC) approaches to predict NO_x in turbulent diffusion jet and recirculating flames. Other work was done by [7] to study NO produced from Hydrogen/air flame using steady and unsteady flamelet approaches to conclude out that steady approach did not give accurate results for NO concentration, whereas, unsteady flamelet modeling obtained accurate results of NO. Lysenko et al. [8] validated the results of Eddy Dissipation Concept approach against experimental data and remarked important enhancement for almost scalars under EDC-based scheme.

As mentioned earlier, the aerodynamic straining imposed by turbulence field strongly affects predicting NO_x reduction. Therefore, adopting a powerful turbulence model is of great significance in estimating NOx characteristics which were done carefully in the present study. However, many numerical studies use RANS, but the intelligence of researchers arises in treating the direct coupling between turbulent mixing and relevant chemistry of NO_x. Many studies in the literature have presented that LES can accurately predict turbulent combustion characteristics of the swirling flow [9–12]. Authors of [13] predicted NO generation in addition consumption for turbulent oxy-combustion using LES scheme [13]. Though, the concentrations of various products haven't been examined against experimental results.

With utilizing air staging, it was observed that (CHi) radicals in rich condition locations have a great impact in a considerable decrease of NO_x concertation [14]. Though, commercial codes don't estimate CHi accurately, specifically with the LES model. Since LES is time-consuming and its computational cost is higher than that of RANS, the detailed kinetics mechanisms are unaffordable for industrial uses, whereas smooth models relied on mixture fraction or chemical equilibrium are extensively used [15–17]. It is useless to exactly evaluate the intermedia species like CHi with the simple chemical kinetics models. Consequently, the simulation of NOx characteristics is not accurate in such applications. A precise empirical NOx scheme with robust turbulence model is required to obtain accurate predictions for industrial uses.

Forgoing studies were performed to develop various techniques to reduce emissions (NO_x and CO). GE accomplished investigations on the improvement of its newest combustor which is employed by AFS technique [18]. Siemens replaced the idea of a "non-premixed pilot nozzle" with a recent scheme based on "premixed pilot nozzle", this scheme is updated to efficiently reduce NO_x characteristics either in low or high-temperature gases [19]. MHPS used V-nozzle type which enhances the mixing strength between air-fuel to keep low-NOx emission characteristics [20]. (AEV) Advanced Environmental Burner, is introduced by Alstom that is based on staging fuel injection and capable to reduce NO_x [21].

Other investigations aim to enhance emission management techniques that utilize catalytic honeycombs to promote the breaking up of NO_x into free Oxygen and Nitrogen. A lot of works have been assigned to the enhancement of SCR "Selective Catalytic Reactors" efficiency [22–24] while others [25, 26] are focusing on the operational techniques to increase the durability and accessibility of such systems. Dilution techniques either by water and steam [27–29], nitrogen [30,31], or carbon dioxide [32,33] to reduce thermal NOx were applied. Exhaust Gas Recirculation (EGR) technique is investigated in [34-36], which returns a percentage of exhaust gas with inlet mixtures. The three methods mentioned earlier should be enhanced and developed with considering all factors that are in charge of stable performance for the combustion system. Chul et al. [37] investigate NOx reduction based on

combustion tuning methodologies optimized by either by F/A ratio or "fuel split ratio". Though, few works were performed as limitations of the adjustment spectrums of such controlling-emissions factors.

The present work examines various combustion and turbulence schemes to select the most accurate models that are capable to predict NO_x and CO emissions and match the experimental measurements published in the literature. Consequently, a parametric analysis is conducted to report the effect of swirl ratio, excess air, diluting fuel with N_2 and CO_2, oxidizer preheating, and oxidizer composition on emissions (NO_x and CO) reduction strategy.

2. Mathematical modelling

The swirl burner studied in the present work is operated with propane fuel. The combustion chamber is configured as 1200 mm in height and 400 mm in diameter with a tapered end at exit having a diameter of 150 mm (see Fig. 1). The burner is assembled from inner fuel and outer air pipes having diameters of 30 and 100 mm respectively, with a vane swirl generator embedded in the annulus.

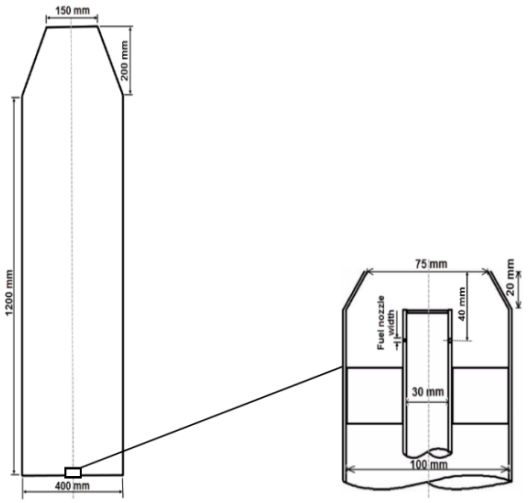

Fig.1. combustion chamber and burner geometry

3. Governing Equations

The physical conservation equations of mass, momentum, energy, and species transport are described in its general form as:

$$\frac{\partial}{\partial x_j}\left(\bar{\rho}\overline{U}_j\Phi + \bar{\rho}\overline{u_j\phi}\right) = \frac{\partial}{\partial x_j}\left[\Gamma_\Phi \frac{\partial \Phi}{\partial x_j}\right] + \bar{\rho}S_\Phi \quad (1)$$

4. Turbulence Models

The present study examined 3 turbulence schemes, namely; "k-ε model, Realizable k-ε model and Reynolds Stress Model (RSM)". Formulation of "turbulence kinetic energy, k" and its "dissipation rate, ε" equations can be expressed as follows:

$$\frac{\partial}{\partial t}(\rho k) + \frac{\partial}{\partial x_j}(\rho k u_j) = \frac{\partial}{\partial x_j}\left[\left(\mu + \frac{\mu_t}{\sigma_k}\right)\frac{\partial k}{\partial x_j}\right] + G_k + G_b - \rho\,\varepsilon - Y_M + S_k \quad (2)$$

$$\frac{\partial}{\partial t}(\rho \varepsilon) + \frac{\partial}{\partial x_j}(\rho \varepsilon u_j) = \frac{\partial}{\partial x_j}\left[\left(\mu + \frac{\mu_t}{\sigma_\varepsilon}\right)\frac{\partial \varepsilon}{\partial x_j}\right] + C_{1\varepsilon}\frac{\varepsilon}{k}(G_k + C_{3\varepsilon}G_b) - C_{2\varepsilon}\rho\frac{\varepsilon^2}{k} + S_\varepsilon \quad (3)$$

In Reynolds Stresses Model RSM, "Reynolds stresses, $\rho\overline{u_i u_j}$ " and "scalar fluxes, $-\rho\overline{u_j\phi}$ are formulated as follows [38]:

$$-\rho\overline{u_i u_j} = \mu_t\left(\frac{\partial \overline{U}_i}{\partial x_j} + \frac{\partial \overline{U}_j}{\partial x_i}\right) - \frac{2}{3}\rho k\delta_{ij} \quad (4)$$

$$-\rho\overline{u_j \phi} = \Gamma_\Phi \frac{\partial \Phi}{\partial x_j} \quad (5)$$

where μ_t is the turbulent viscosity and Γ_Φ is equal to μ_t/σ_Φ. The turbulent viscosity is modeled as

$$\mu_t = c_\mu \rho f_\mu K^2/\varepsilon \quad (6)$$

where c_μ, f_μ and σ_Φ are constants. The turbulent viscosity is thus obtained from the solution of the transport equations for k and ε.

5. Combustion Models

Combustion inside the chamber was carried out by using three different models, namely; "Eddy Dissipation model", "PDF-based Equilibrium model" and "PDF-based Flamelet model".

(a) Eddy Dissipation Model (EDM)

It assumes very fast reaction and its kinetics is only dominated by turbulent mixing. Reaction rate can be expressed as follows:

$$\overline{R}_f = A\rho\frac{\varepsilon}{k}\min\left(\overline{Y}_f, \frac{1}{\nu}\overline{Y}_o, B\frac{1}{1+\nu}\overline{Y}_p\right) \quad (7)$$

(b) PDF-based Equilibrium Model

EDM calculates the average values of scalar variables, where mean values *G* could be expressed in equation (8) and f (ξ) is the probability density function

$$\overline{G} = \int_{-\infty}^{\infty} G(\xi) f(\xi)\, d\xi \quad (8)$$

(c) PDF Flamelet Model

In Flamelet Approach, mapped equations of species and temperature in "mixture fraction, *f*" domain are expressed as follows;

$$\rho\frac{\partial Y_i}{\partial t} = \frac{1}{2}\rho\chi\frac{\partial^2 Y_i}{\partial f^2} + S_i \quad (9)$$

$$\rho\frac{\partial T}{\partial t} = \frac{1}{2}\rho\chi\frac{\partial^2 T}{\partial f^2} - \frac{1}{c_p}\sum_i H_i S_i + \frac{1}{2c_p}\rho\chi\left[\frac{\partial c_p}{\partial f} + \sum_i c_{p,i}\frac{\partial Y_i}{\partial f}\right]\frac{\partial T}{\partial f} \quad (10)$$

where, *f*, c_{pi}, c_p, H_i and S_i are mixture fraction, the specific heat of component i, mixture-average specific heat, specific enthalpy of component i and reaction rate of species i, respectively.
"Scalar dissipation rate, χ ", is termed in eq. (11) as follows;

$$\chi(f) = \frac{a_s}{4\pi}\frac{3\left(\sqrt{\rho_\infty/\rho}+1\right)^2}{2\sqrt{\rho_\infty/\rho}+1}\exp\left(-2\left[erfc^{-1}(2f)\right]^2\right) \quad (11)$$

"Probability Density Function, *p(f)*" can be written mathematically in eq. (12) as follows;

$$p(f)\,\Delta f = \lim_{T\to\infty}\frac{1}{T}\sum_i \tau_i \quad (12)$$

(d) NOx Formation Model

The reduced reaction mechanism that formulates the production of NOx is expressed as [39]:

$$O + N_2 \underset{k-1}{\overset{k1}{\Longleftrightarrow}} N + NO \quad (13)$$

$$O_2 + N \underset{k-2}{\overset{k2}{\Longleftrightarrow}} O + NO \quad (14)$$

Conserving NO species is evaluated from

$$\frac{\partial}{\partial x_j}(\rho U_j Y_{NO}) = \frac{\partial}{\partial x_j}\left[\Gamma_{NO}\frac{\partial Y_{NO}}{\partial x_j}\right] + S_{NO} \quad (15)$$

"Source term of NO, S_{NO}" is calculated from eq. (16) & (17)

$$\frac{d(NO)}{dt} = \frac{2[O](k_1 k_2 [O_2][N_2] - k_{-1}k_{-2}[NO]^2)}{k_2[O_2] + k_{-1}[NO]} \quad (16)$$

$$S_{NO,thermal} = M_{NO}\frac{d(NO)}{dt} \quad (17)$$

The specific reaction rate constants for the NO_x model are obtained as [39]:

$$k_1 = 1.8 \times 10^8 \exp(-38370/T) \quad (18)$$

$$k_{-1} = 3.8 \times 10^7 \exp(-425/T) \quad (19)$$

$$k_2 = 1.8 \times 10^4 T \exp(-4680/T) \quad (20)$$

$$k_{-2} = 3.8 \times 10^3 T \exp(-20820/T) \quad (21)$$

The turbulence manner causes time-based variations corresponding to concentrations and temperature that affects the reaction rates of kinetics mechanism. Then, using temporal averaging for concentrations and temperature to estimate NO_X will produce considerable deviation in its prediction. In this study, PDF model will consider time-based variations corresponding to concentrations and temperature as a result of turbulence, hence accurate estimation of reaction rates and NOx concentration as well has been obtained.

6. Radiation Model

As mentioned above, the "P-1 radiation model" is adopted for the present case study to consider radiation resulted from the flame and to show its effect on NOx production. The "radiation flux, q_r" is expressed in eq. (22).

$$q_r = -\frac{1}{3(a+\sigma_s) - C\sigma_s}\nabla G \quad (22)$$

$$\Gamma = \frac{1}{(3(a+\sigma_s) - C\sigma_s)} \quad (23)$$

After defining Γ as the parametric term multiplied by ∇G , Eq. (22) could be reduced to

$$q_r = -\Gamma \nabla G \quad (24)$$

The transport form of G could be expressed as

$$\nabla \cdot (\Gamma \nabla G) - aG + 4an^2\sigma T^4 = S_G \quad (25)$$

where *"n*, the refractive index of the medium", "σ is the Stefan-Boltzmann constant" and "S_G is a user-defined radiation" source. Gathering eq. (24) and (25) leads to:

$$-\nabla \cdot q_r = aG - 4an^2\sigma T^4 \quad (26$$

The expression for $-\nabla \cdot q_r$ can be directly substituted into the energy equation to account for heat sources (or sinks) due to radiation.

7. Numerical Modelling

After performing grid sensitivity analysis between different numbers of cells, it has been observed that 45,000 cells have better results with low computational efforts needed. The axisymmetric assumption eases solving the present study by reducing 50% of the computational domain (see Fig.2). The numerical solution is based on steady state pressure based implicit 2-D swirl solver using 2nd order scheme. The convergence criteria for the iterative solution is enabled to be 10^{-6} for both radiation and energy equations however for the remaining equations, it is identified to be 10^{-4}.

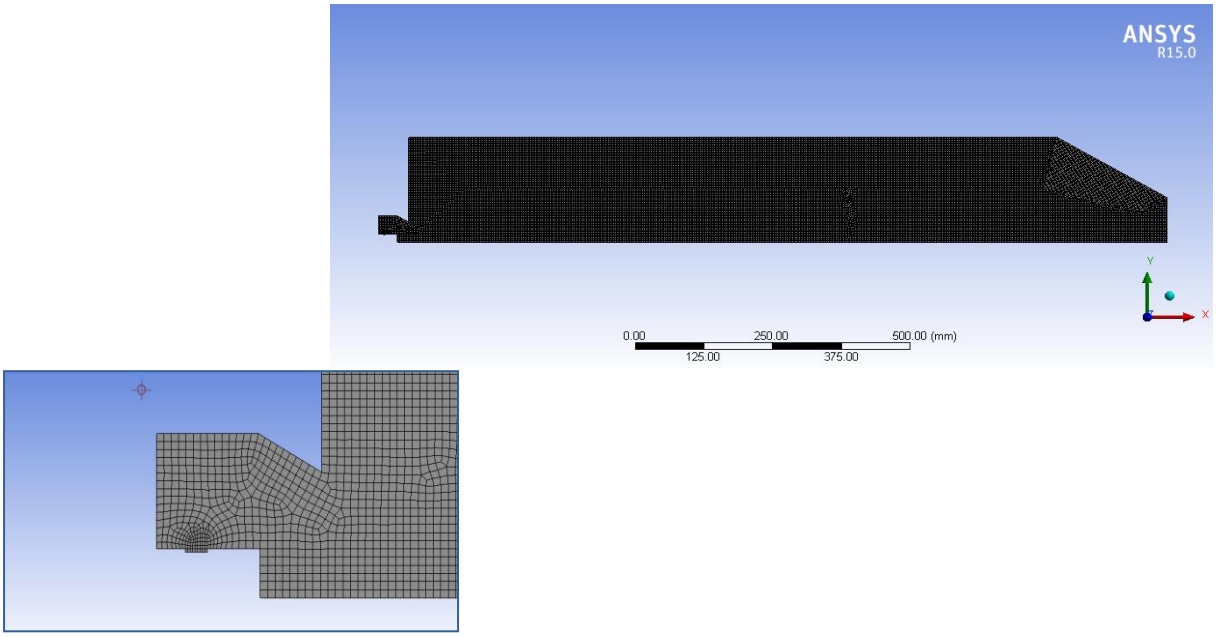

Fig.2. Grid structure inside the solution domain.

7.1. Evaluation of Turbulence Models

In order to select the best turbulence scheme which gives accurate results with appropriate computational efforts, a number of turbulence schemes was tested for various runs of non-reacting flow with severe swirling. The present test examines the validity of k-ε, realizable k-ε and Reynolds stress (RSM) models where figure 3 compares the predicted axial velocities for the three tested turbulence schemes at different axial sections. At lower axial sections, there is a large contradiction between the profiles of axial velocities since k-ε model obtains lower maximum axial velocity compared to realizable k-ε and RSM. Moreover, the position of maximum axial velocity is located at higher radial distance for k-ε model and at lower radial distance for realizable k-ε but RSM located it between the extreme positions of of k-ε and realizable k-ε. Along higher axial sections, the swirling effect diminishes leading to great coincidence between the three profiles of axial velocities. The significance of the turbulence model rises

in its potential to perfectly predict the recirculation zones and vortices inside the swirling flow with reasonable computational efforts which leads us to choose RSM model among other turbulence models.

7.2. Evaluation of Combustion Models

In an analogous approach, three different combustion models, namely; "Eddy Dissipation" model, "Equilibrium PDF" model, and "Flamelet PDF" model are examined. The turbulence scheme adopted for this comparison is RSM as mentioned earlier. As depicted from figure 4, EDC model fails to predict the reverse flow structure resulted from induced recirculation of hot products which misleads the flame profile and gives high temperatures. On the contrary, the other two models of PDF give realistic values of temperature because of their great capabilities to predict the recirculation nature and involve more reactive species when compared to EDC model. Even with the great similarity between equilibrium PDF and Flamelet PDF in predicting the temperature contours but Flamelet PDF model is preferred for its potential to consider non-equilibrium variations in turbulent flames resulted from aerodynamic straining. Consequently, Flamelet PDF model is chosen to be the combustion model of the present case study.

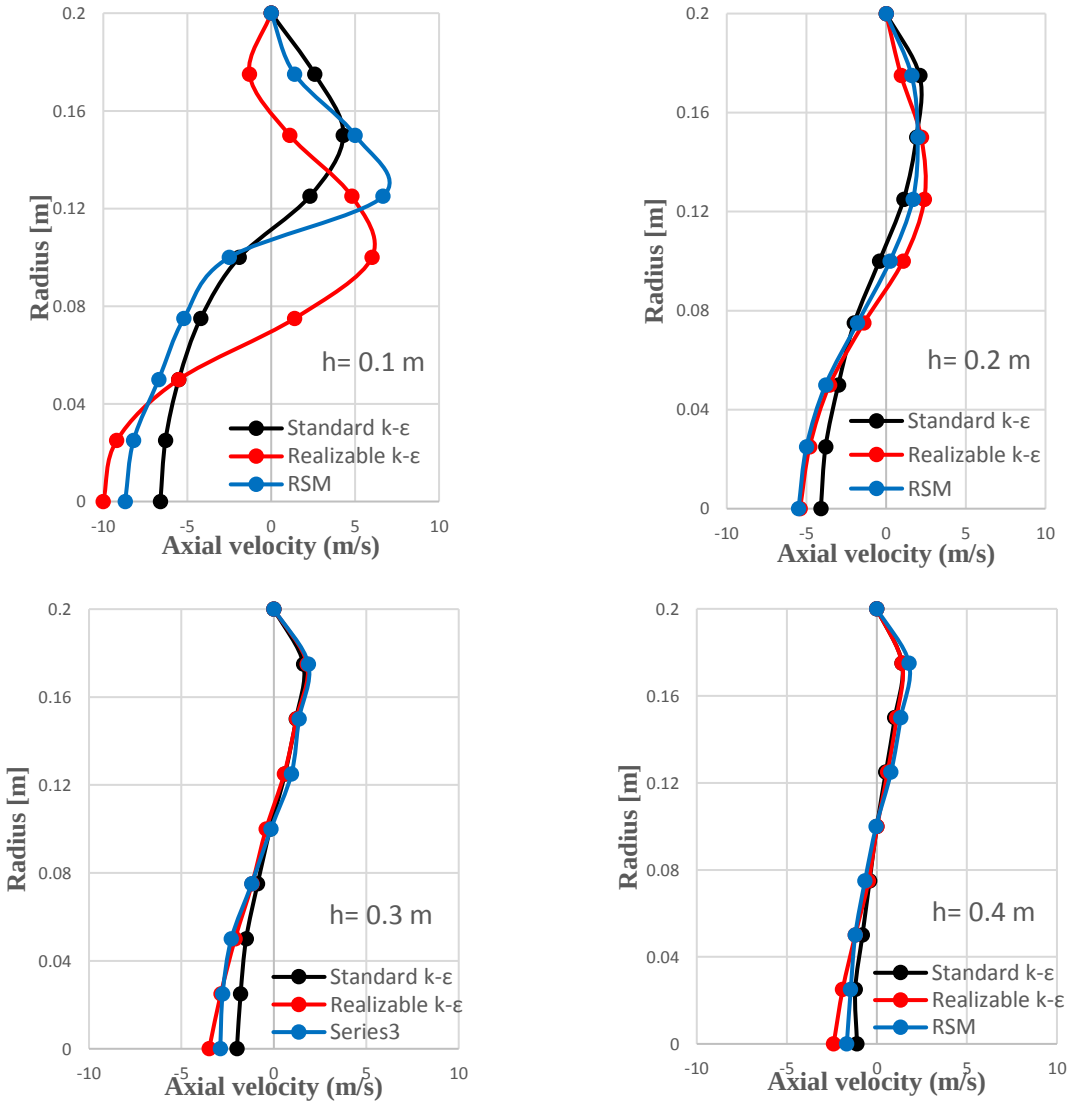

Fig. 3. Mean axial velocities at various positions above the burner (h) using the standard k-ε model, the realizable k-ε model and the RSM for cold flow.

(a) Eddy Dissipation Concept, EDC model

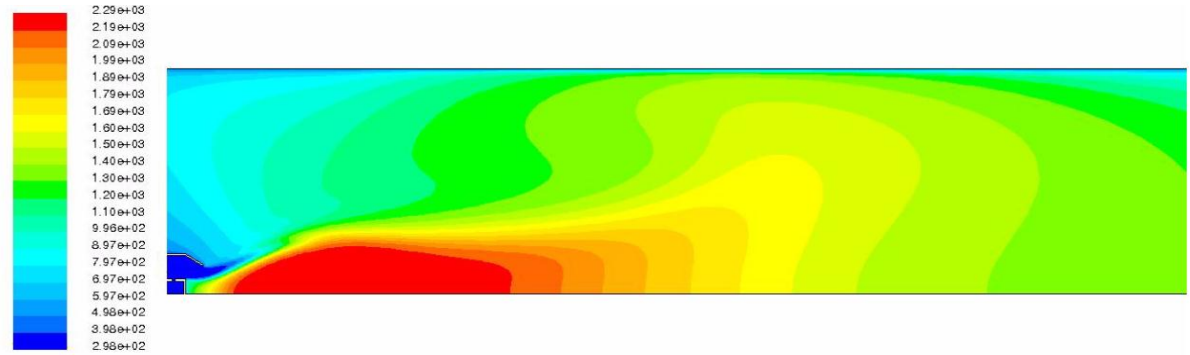

(b) Equilibrium PDF

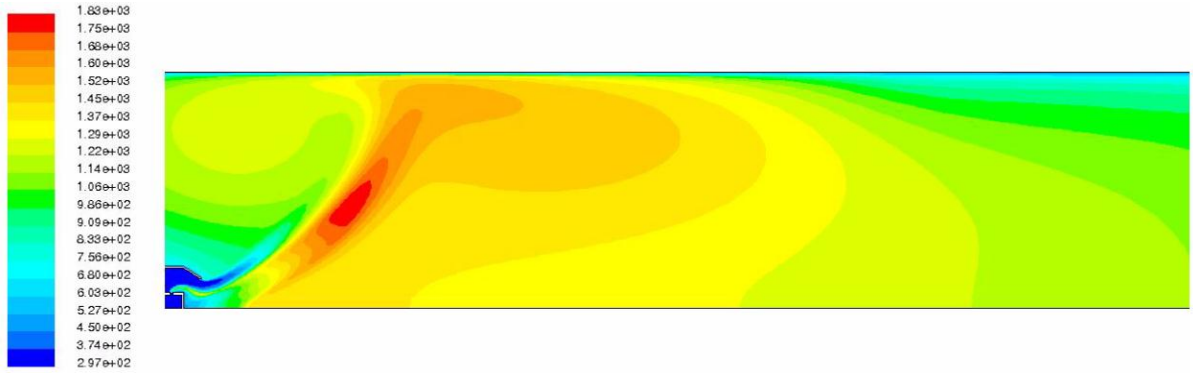

(c) Flamelet PDF

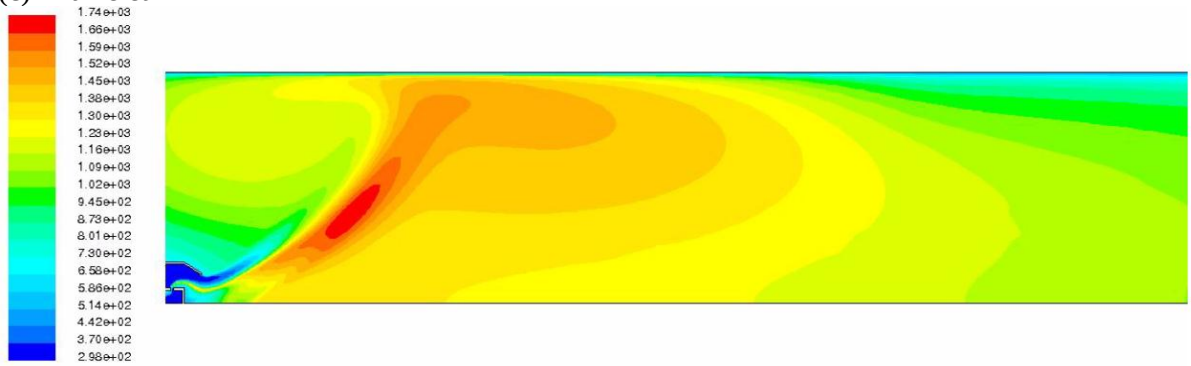

Fig. 4. Temperature contours inside the chamber; (a) Eddy Dissipation Concept (EDC) model; (b) Equilibrium PDF model ; (c) Flamelet PDF model.

7.3. Validation with Experiments

NOx data for the present study which was done by using the grid of 45,000 cells, RSM as the turbulence model and Flamelet model as the combustion model, are compared with the experimental results of Øystein [40] for power range (80-240 kW).

8. Results

In this section, a parametric study demonstrating the effect of swirl ratio, excess air, diluting fuel with N_2 and CO_2, oxidizer preheating, and oxidizer composition on NO_x and CO emissions are carried out and described. The influence of swirling degree on (NO_x and CO) mole fractions and peak flame temperature at the combustion chamber exit is presented in figure 6.

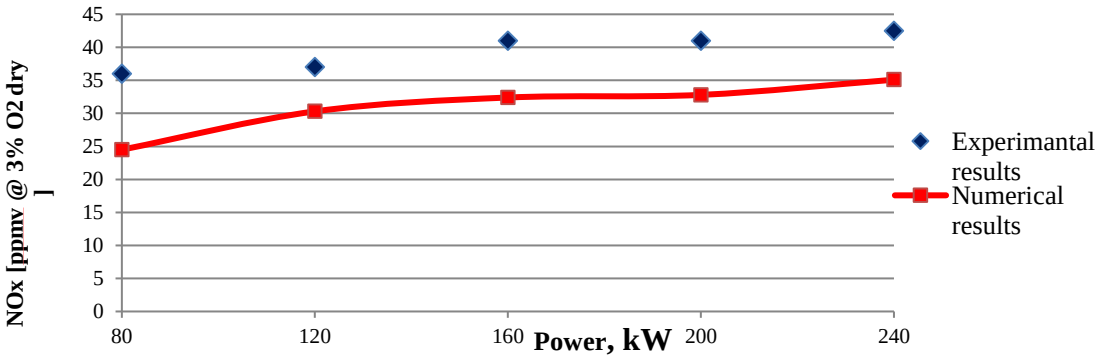

Fig. 5. Comparison between predicted and measured concentrations of NOx

It is observed that NOx and CO mole fractions are reduced as the swirling degree increases, this is could be explained as a result of decreasing the peak flame temperature with rising the swirling degree. This outcome justifies the major impact of lowering flame temperature on reducing thermal NOx mechanism and CO dissociation. The peak flame temperature is lowered with rising the swirling degree because of entraining more amounts of the recirculated flue gases into the central toroidal recirculation zone CTRZ which inhibits the chemical reaction rates and reduces the flame temperature as well.

Figure 7 presents the variation of (NOx and CO) mole fractions and peak flame temperature with excess air factor (EAF) at the outlet section of the combustion chamber. As shown, NOx concentration increases by increasing EAF from 0% to 5%, although the peak flame temperatures are invariant in this range. This abnormal observation leads us to carry out a simulation of temperature contour along the whole chamber for the two cases of EAF as presented in figure 8. It is obviously clear that the flame surface region of 5% EAF is wider than that of the stoichiometric case (EAF = 0), which means that the hot surface areas at 5% EAF is larger than their counterparts at 0% EAF and that leads to generate more NOx at 5% EAF than at 0% EAF. While the CO emissions decrease through the same range of EAF (0% - 5%) due to the existence of a large amount of oxygen at higher EAF. Above 5 % EAF, it is shown that both NOx and CO concentration decrease with increasing EAF because of continuous decrease of peak flame temperature for the same range of EAF.

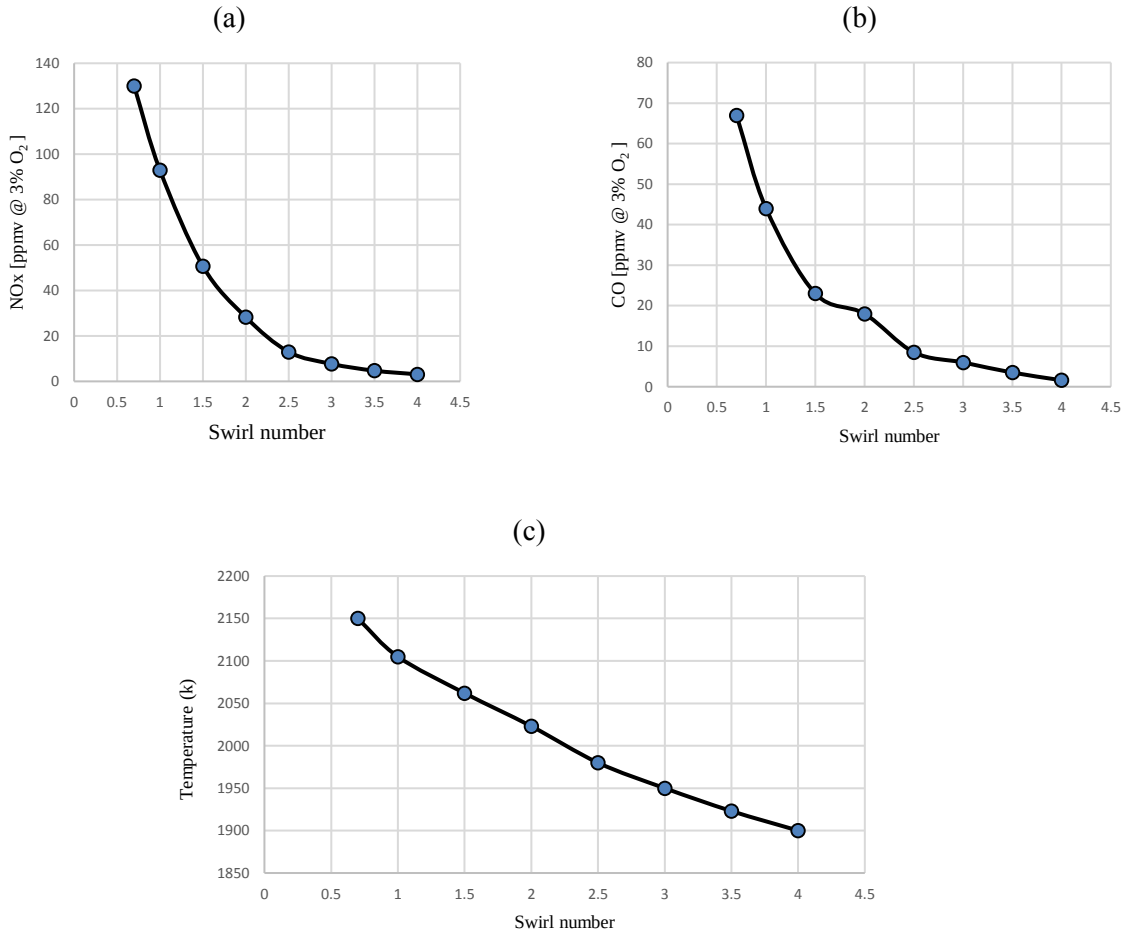

Fig. 6. Effect of varying swirling degree on (a) NO_x mole fraction, (b) CO mole fraction, and (c) peak flame temperature

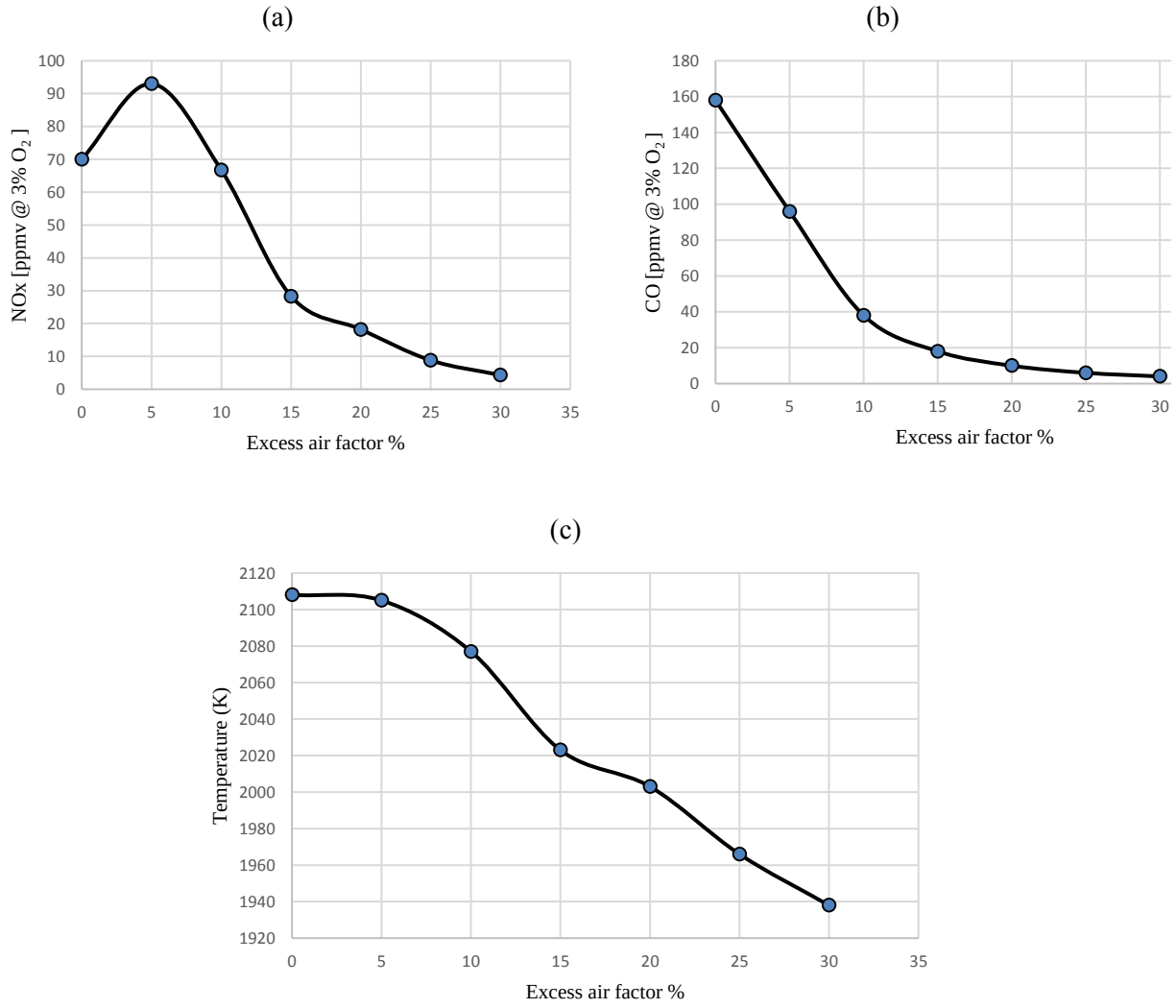

Fig. 7. Effect of varying excess air factor (EAF) on (a) NO_x mole fraction, (b) CO mole fraction, and (c) peak flame temperature

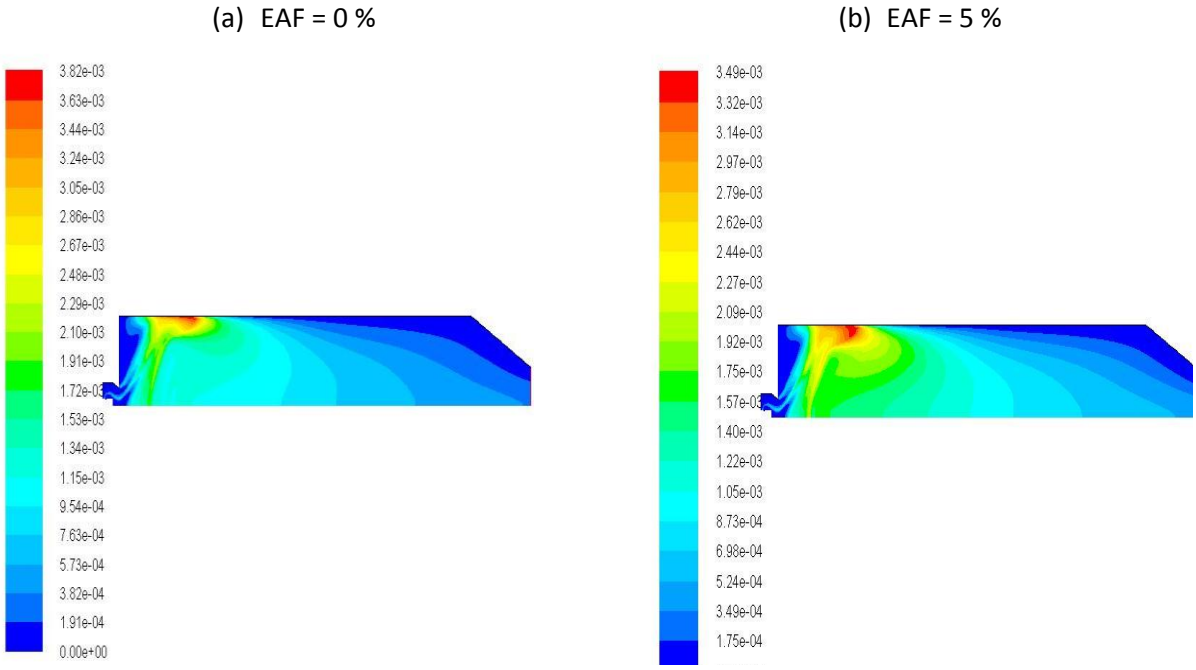

Fig. 8 Distribution of flame temperature contours for (a) EAF=0% and (b) EAF=5%

Mixing the fuel with N_2 as a diluent (inert gas that does not contribute in the combustion reactions but behaves as a heat sink) lowers the peak flame temperature. Figure 9 shows the variation of (NO_x and CO) emissions and peak flame temperature at different Diluent to Fuel Ratio (DFR) [mass basis]. It is observed that NO_x and CO mole fractions decrease with the increase of DFR due to a decrease in the peak flame temperature with increasing DFR. As mentioned previously the thermal NO_x mechanism and CO dissociation depend directly on the peak flame temperature. This reduction in the peak flame temperature is caused by increasing the amount of the diluent gas presented in the primary combustion chamber zone.

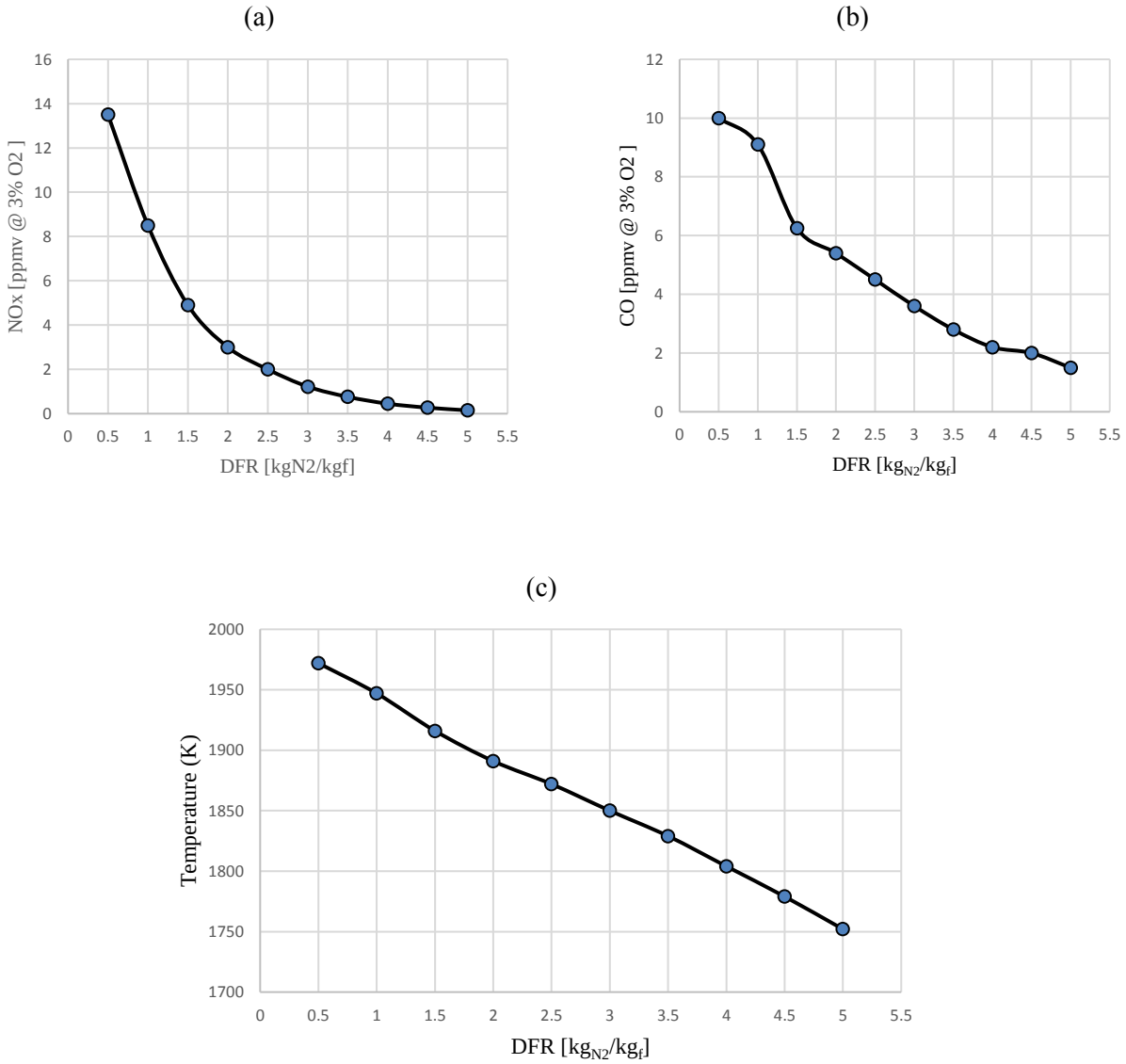

Fig. 9. Effect of varying diluent fuel ration (DFR) on (a) NO_x mole fraction, (b) CO mole fraction, and (c) peak flame temperature

Preheating of combustion air is one of the most popular uses of recovered heat from exhaust gases and due to its high efficiency and reduction in primary fuel use. The influence of changing the preheating temperature on (NO_x and CO) emissions and peak flame temperature at outlet section are shown in figure 10. It is depicted that NO_x and CO mole fractions increase with increasing the preheating temperature due to rising the peak flame temperature, where NO_x emissions increase exponentially with preheating temperature increase

.

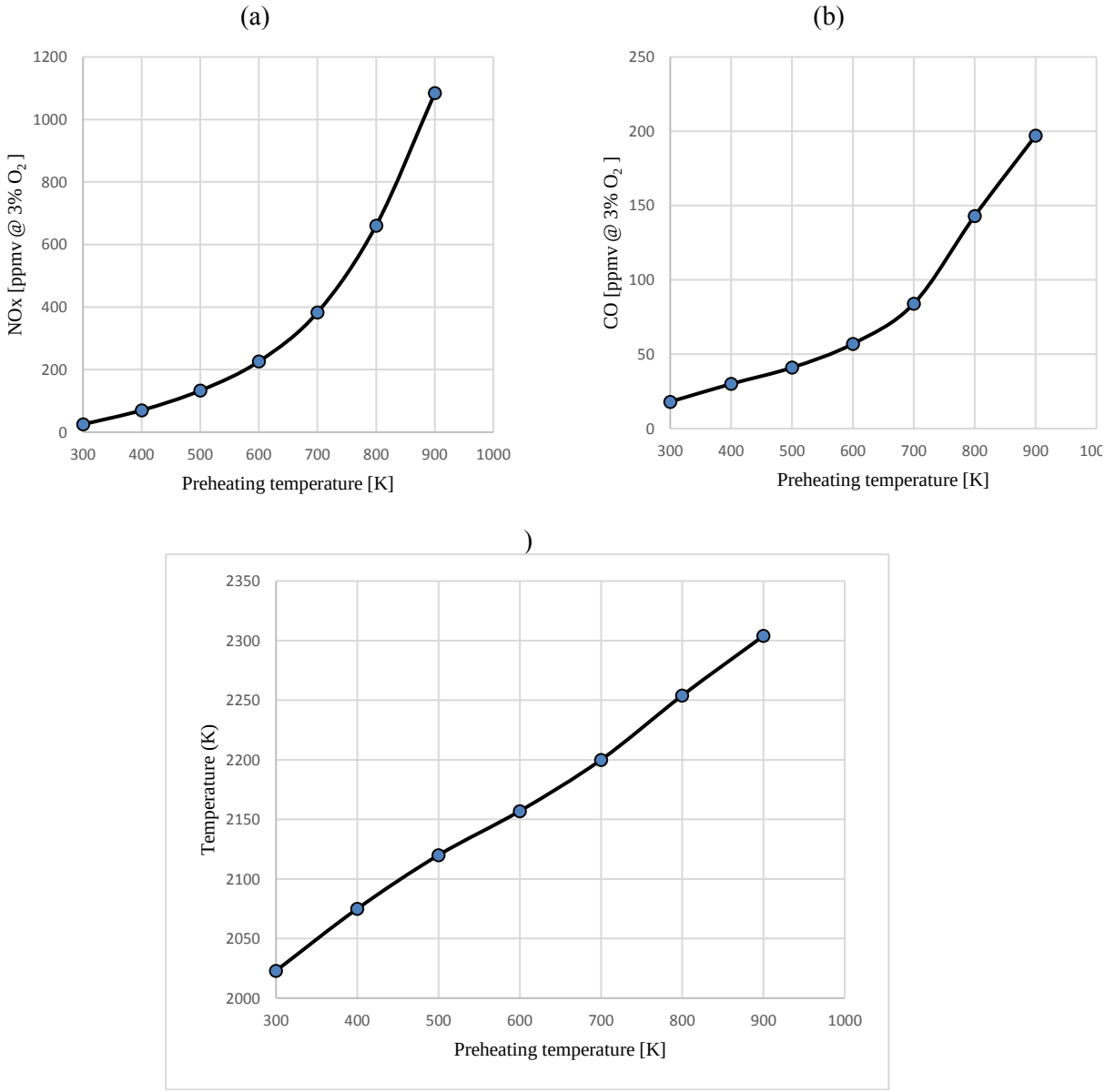

Fig. 10. Effect of varying preheating temperature on (a) NO_x mole fraction, (b) CO mole fraction, and (c) peak flame temperature

Air (21% O_2 & 79% N_2) is the main oxidizer used in many combustion applications. In the present investigation, different percentages of oxygen and nitrogen have been composed to study its constituent variation on NOx and CO mole fractions. As presented in figure 11, NOx emissions rise 8 times of its value with increasing the oxygen composition in the main oxidizer from 21% to 80%. This is justified with the increase of peak flame temperature with increasing oxygen concentration. It is also noticed that, NOx concentration sharply decays after reaching its peak value at Oxygen concentration of 80%, since there is an insufficient amount of nitrogen in the oxidizer to form NOx. In the other side, CO emissions continuously increase with oxygen concentration increase because of the noticeable rise in the peak flame temperature as illustrated in figure 11.

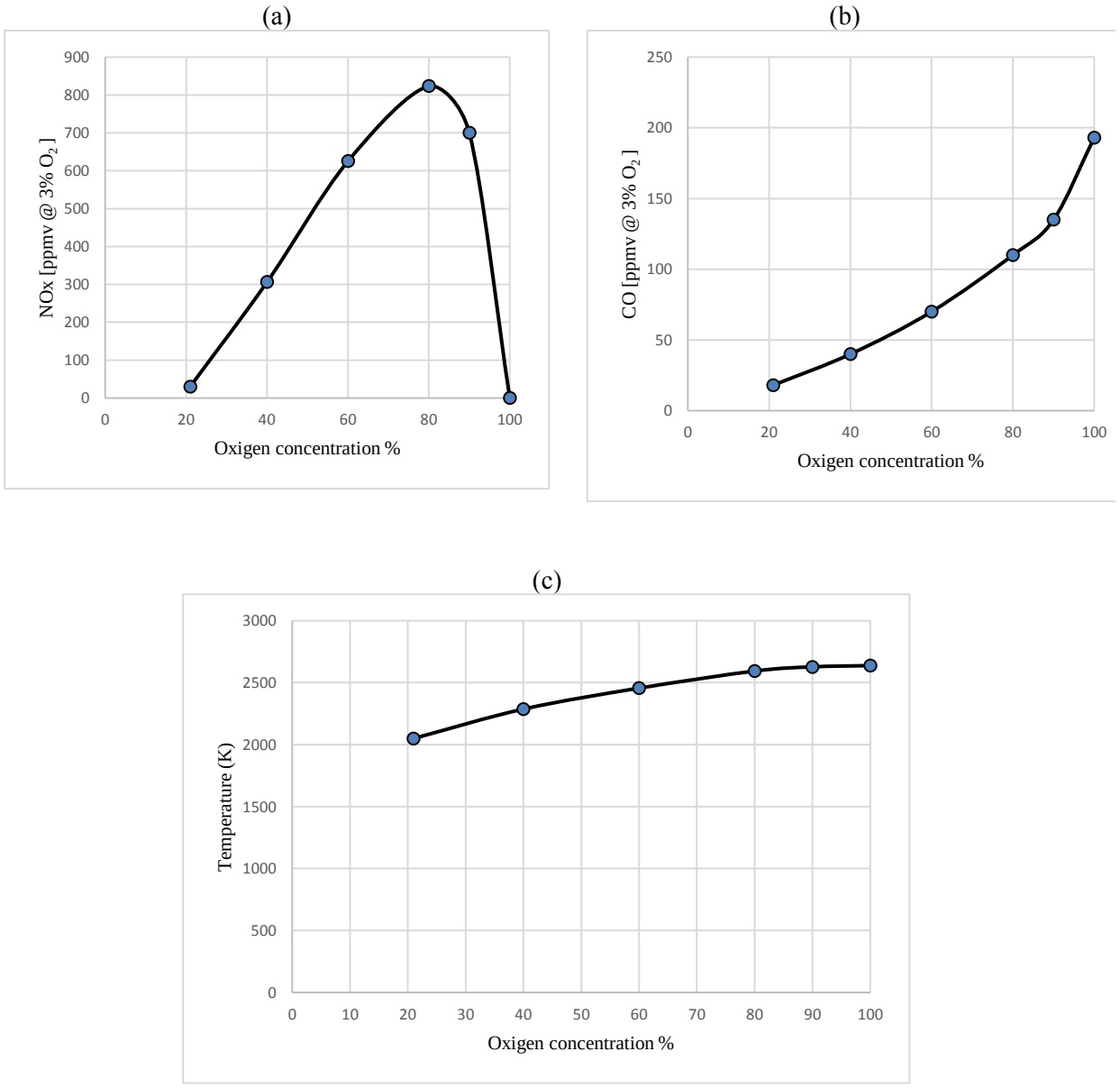

Fig. 11. Effect of varying Oxygen concentration on (a) NO_x mole fraction, (b) CO mole fraction, and (c) peak flame temperature

9. Conclusions

The present work tested different combustion and turbulence models to select the appropriate models that are capable to accurately predict emission characteristics issued from combustion chamber. The analysis showed that the combination of RSM turbulence model with PDF-flamelet combustion model is the best choice that shows a great agreement with experimental data. The effect of varying swirl ratio, excess air, diluting fuel with N_2 and CO_2, oxidizer preheating, and oxidizer composition on emissions (NO_x and CO) reduction strategy concluded that increasing the swirl number, excess air factor, and (N_2 and CO_2) mixing ratios have a positive effect on NOx and CO emissions reduction. While increasing the preheating temperature, and the oxidizer Oxygen concentration leads to an increase the NOx and CO emissions.

References

[1] Szodruch, J., "Technological targets for future air transportation in europe, panel presentations", ISABE 2005, Munich (September 2005).
[2] Chen, J.Y., Chang, W.C., Koszykowski, M., "Numerical simulation and scaling of NOx emissions from turbulent hydrogen jet flames with various amounts of helium dilution", Combust. Sci. Technol. 110 (1) (1995) 505-529.
[3] Chen, J.Y., Kollmann, W., "PDF modeling and analysis of thermal NO formation in turbulent nonpremixed hydrogen-air jet flames", Combust. Flame 88(3-4) (1992) 397-412
[4] Yadav, R., Nakod, P., Rajeshirke, P., " NO Prediction in Turbulent Diffusion Flame Using Multiple Unsteady Laminar Flamelet Modeling", ASME J. Eng. Gas Turb. Power 136(10) (2014) 101515.
[5] Sanders, J.P.H., Chen, J.Y., Gökalp, I., "Flamelet-based modeling of NO formation in turbulent hydrogen jet diffusion flames", Combust. Flame 111(1-2) (1997) 1-15.
[6] Kim, G., Kang, S., Kim, Y., Bilger, R.W., Cleary, M.J., "Conditional moment closure and transient flamelet modelling for detailed structure and NO x formation characteristics of turbulent nonpremixed jet and recirculating flames', Combust. Theor. Model. 11(4) (2007) 527-552.
[7] Pitsch, H., Chen, M., Peters, N., "Unsteady flamelet modeling of turbulent hydrogen-air diffusion flames", Proc. Combust. Inst. 27(1) (1998) 1057-1064.
[8] Lysenko, D.A., Ertesvåg, I.S., Rian, K.E. "Numerical simulations of the sandia flame d using the eddy dissipation concept", Flow Turbul. Combust. 93(4) (2014) 665-687.
[9] Chen L, Ghoniem AF. Simulation of oxy-coal combustion in a 100 kWth test facility using RANS and LES: a validation study. Energy Fuels 2012;26(8):4783–98.
[10] Yamamoto K, Murota T, Okazaki T, et al. "Large eddy simulation of a pulverized coal jet flame ignited by a preheated gas flow". Proc Combust Inst 2011;33(2):1771–8.
[11] Warzecha P, Boguslawski A. "LES and RANS modeling of pulverized coal combustion in swirl burner for air and oxy-combustion technologies". Energy 2014;66:732–43.
[12] Olenik G, Stein OT, Kronenburg A. "LES of swirl-stabilised pulverised coal combustion in IFRF furnace" No. 1. Proc Combust Inst 2015;35(3):2819–28.
[13] Muto M, Watanabe H, Kurose R, et al. "Large-eddy simulation of pulverized coal jet flame–effect of oxygen concentration on NOx formation". Fuel 2015;142:152–63.
[14] Taniguchi M, Kamikawa Y, Okazaki T, et al. "A role of hydrocarbon reaction for NOx formation and reduction in fuel-rich pulverized coal combustion". Combust Flame 2010;157(8):1456–66.
[15] Wen X, Luo K, Luo Y, et al. "Large eddy simulation of a semi-industrial scale coal furnace using non-adiabatic three-stream flamelet/progress variable model" J. Appl Energy 2016;183:1086–97.
[16] Rieth M, Proch F, Clements AG, et al. "Highly resolved flamelet LES of a semi-industrial scale coal furnace". Proc Combust Inst 2017;36(3):3371–9.
[17] Pedel J, Thornock JN, Smith PJ. "Ignition of co-axial turbulent diffusion oxy-coal jet flames: experiments and simulations collaboration". Combust Flame 2013;160(6):1112–28.
[18] Cerutti Matteo, Giannini Nicola, Ceccherini Gianni, Meloni Roberto, Matoni Emanuele, Romano Christian, Riccio Giovanni. "Dry low nox emissions operability enhancement of a heavy-duty gas turbine by means of fuel burner design development and testing. Proceedings of ASME Turbo Expo. 2018. GT2018-76587.
[19] Kock Boris F, Prade Bernd, Witzel Benjamin, Streb Holger, Koenig Mike H. "Combustion system update SGT5-4000F – design, testing & validation". Proceedings of ASME Turbo Expo. 2013. GT2013-95569.
[20] Tanimura Satoshi, Nose Masakazu, Ishizaka Koichi, Takiguchi Satoshi, Rodriguez Jose. Advanced "dry low NOx combustor for MITSUBISHI G class gas turbines". Proceedings of ASME Turbo Expo 2008 2008. p. 2008.

[21] Bothien Mirko R, Pennell Douglas A, Zajadatz Martin, Döbbeling Klaus. "On key features of the aev burner engine implementation for operational flexibility". Proceedings of ASME Turbo Expo. 2013. GT2013-95693.
[22] Jodłowski PJ, Kryca J, Rogulska A, Gil B, Iwaniszyn M, Łojewska J, et al. "Advantages of a wire gauze structured reactor with a zeolite (Cu-USY) catalyst for NH3-SCR of NOx". Chem Eng J 2013;214:319–26.
[23] Costa Costas N, Savva Petros G, Fierro José Luis G, Efstathiou Angelos M. "Industrial H2-SCR of NO on a novel Pt/MgO–CeO2 catalyst". Appl Catal B, 75. 2007. p.147–56.
[24] Forzatti Pio. "Present status and perspectives in de-NOx SCR catalysis". Appl Catal A 2001;222:221–36.
[25] Liang Zengying, Ma Xiaoqian, Lin Hai, Tang Yuting. "The energy consumption and environmental impacts of SCR technology in China". Appl Energy 2011;88:1120–9.
[26] Kobayashi Motonobu, Miyoshi Katsunori. "WO3–TiO2 monolithic catalysts for high temperature SCR of NO by NH3: influence of preparation method on structural and physico-chemical properties, activity and durability". Appl Catal B 2007;72:253–61.
[27] Xue Rui, Chunbo Hu, Sethi Vishal, Nikolaidis Theoklis, Pilidis Pericle. :Effect of steam addition on gas turbine combustor design and Performance:. Appl. Therm. Eng. 2016;104:249–57.
[28] Farokhipour A, Hamidpour E, Amani E. "A numerical study of NOx reduction by water spray injection in gas turbine combustion chambers. Fuel 2018;212:173–86.
[29] Amani E, Akbari MR, Shahpouri S. "Multi-objective CFD optimizations of water spray injection in gas-turbine combustors". Fuel 2018;227:267–78.
[30] Li Shan, Hua Zhou, Hou Lingyun, Ren Zhuyin. "An analytic model for the effects of nitrogen dilution and premixing characteristics on NOx formation in turbulent premixed hydrogen flames". Int J Hydrogen Energy 2017;42:7060–70.
[31] Lee In Bok, Woo In Sung, Lee Min Chul. "Effects of nitrogen dilution on the NOx and CO emission of H2/CO/CH4 syngases in a partially-premixed gas turbine model combustor". Int J Hydrogen Energy 2016;41:15841–51.
[32] Lee Kangyeop, Kim Hyungmo, Park Poomin, Yang Sooseok, Ko Youngsung. "CO2 radiation heat loss effects on NOx emissions and combustion instabilities in lean premixed flames". Fuel 2013;106:682–9.
[33] Best Thom, Finney Karen N, Ingham Derek B, Pourkashanian Mohamed. "Impact of CO2-enriched combustion air on micro-gas turbine performance for carbon capture". Energy 2016;115:1138–47.
[34] Ditarantoa Mario, Li HaCng, Løvas Terese. "Concept of hydrogen fired gas turbine cycle with exhaust gas recirculation: assessment of combustion and emissions performance". Int J Greenhouse Gas Control 2015;37:377–83.
[35] Evulet Andrei T, ELKady Ahmed M, Brand Anthony R, Chinn Daniel. "On the performance and operability of GE's dry low NOx combustors utilizing exhaust gas recirculation for post-combustion carbon capture". Energy Proc 2009;1:3809–16.
[36] Liu Zuming, Karimi Iftekhar "A. New operating strategy for a combined cycle gas turbine power plant". Energy Convers Manage 2018;171:1675–84.
[37] Lee Min Chul, Chung Jae Hwa, Park Won Shik, Park Seik, Yoon Youngbin. "The combustion-tuning methodology of an industrial gas turbine using a sensitivity analysis". Appl Therm Eng 2012.
[38] Wilcox D.C. Turbulence Modeling for CFD. DCW Industries; 2010.
[39] Handby V., Li G., "Modeling of Thermal Emissions Performance of Commercial Boilers," Ventilation Air-Conditioning and Refrigeration Journal 2007;3(2):101–11.
[40] Øystein, S., "Experimental and Theoretical Studies of a Low NOx Swirl Burner," phD Thesis, Department of Energy and Process Engineering, The Norwegian University of Science and Technology, 2004.